Mid-infrared 333-MHz frequency comb continuously tunable from 1.95 – 4.0 µm

Mid-infrared 333-MHz frequency comb continuously tunable from 1.95 – 4.0 µm

Karolis Balskus,* Zhaowei Zhang, Richard A. McCracken, and Derryck T. Reid

Scottish Universities Physics Alliance (SUPA), Institute of Photonics and Quantum Sciences, School of Engineering and Physical Sciences, Heriot-Watt University, Riccarton, Edinburgh EH14 4AS, UK
**Corresponding author: kb202@hw.ac.uk*

Received XX Month XXXX; revised XX Month, XXXX; accepted XX Month XXXX; posted XX Month XXXX (Doc. ID XXXXX); published XX Month XXXX

We report a 333-MHz femtosecond optical parametric oscillator in which carrier-envelope offset stabilization was implemented by using a versatile locking technique that allowed the idler comb to be tuned continuously over a mid-infrared range from 1.95 µm to 4.0 µm. A specially designed multi-section and multi-grating periodically-poled KTP crystal provided simultaneously phasematched parametric down-conversion and pump + idler sum-frequency generation, enabling strong heterodyne signals with the pump super-continuum (employed for locking) to be obtained across the tuning range of the device. The idler comb offset was stabilized to a 10-MHz reference frequency with a cumulative phase noise from 1 Hz–64 kHz of <1.3 rad maintained across the entire operating range, and average idler output powers up to 50 mW.

OCIS Codes: (320.7110) Ultrafast nonlinear optics; (190.4970) Parametric oscillators and amplifiers; (140.3425) Laser stabilization; (120.3930) Metrological instrumentation.

http://dx.doi.org/10.1364/OL.99.099999

Mid-infrared (mid-IR) frequency combs in the 3–5 µm region are promising sources for dual-comb [1] and coherent FTIR spectroscopy [2] and for molecular spectroscopy / trace gas detection [3, 4]. Combs producing longer wavelengths could have applications in laser-driven particle acceleration [5] or as sources of carrier-envelope-phase (CEP) stabilized seed pulses for injection into high power amplifiers [6, 7] for extreme ultraviolet (XUV) high harmonic generation [8,9].

Several approaches have previously been applied to practically realize mid-infrared combs. Difference frequency generation (DFG) has been used to create combs extending from 3–17 µm, with high-power Er:fibre laser pumping enabling >100 nW [10–12] per comb line, however with only low efficiency. Comb generation from high-Q-factor optical micro-resonators [13, 14], in which four-wave mixing generates signal and idler combs from an intense CW pump, has been extended to 2.5 µm in MgF_2 [15] and up to 3.1 µm using silicon [16]. Mid-IR micro-resonator combs, while a very promising technology, remain under intensive investigation, as the combs they produce can be highly structured and can vary considerably in their coherence properties. Femtosecond lasers emitting light directly in the mid-IR have also been reported, notably Cr^{2+}:ZnSe [17,18], Cr^{2+}:ZnS [19] and Tm-/Ho-co-doped fiber lasers [20] operating from 2.0-2.4 µm, and fully stabilized frequency combs have been demonstrated from such systems [21,22]. In comparison with the above mentioned technologies, optical parametric oscillators (OPOs) currently represent the highest average power and most efficient sources of mid-IR combs [23], with wavelengths extending to 4.8 µm [23, 24] and instrument-limited comb linewidths of ~15 Hz being achieved [25]. Details on the tuning flexibility of the OPO frequency-combs reported in the literature are scarce, however degenerate OPOs have been reported which emit spectra instantaneously covering 900 cm^{-1} at 3 µm [26].

In this Letter we describe a fully-stabilized mid-IR OPO frequency comb with a broadly tunable output spanning from 1.95 µm to 4.0 µm, in which both the pump repetition rate and the carrier-envelope offset (CEO) frequency of the idler pulses are locked to a traceable radio-frequency reference. Illustrated in Fig. 1, the OPO was a 4-mirror ring cavity based on a cascaded-grating PPKTP crystal (Raicol Crystals) and synchronously-pumped by a 333 MHz Ti:sapphire laser (Gigajet, Laser Quantum) producing pulses with durations of 30 fs and an average power of 1.5 W. All mirrors had high reflectivity from 980–1620 nm (signal) and high transmission from 750–850 nm (pump) and 1700–5000 nm (idler).

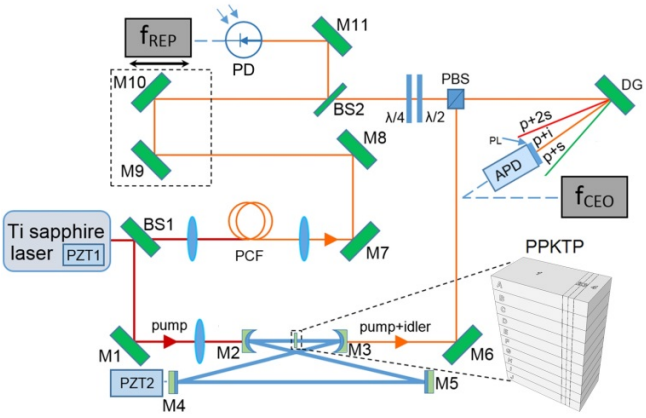

Fig. 1. Layout of the PPKTP OPO: OC, output coupler; PD, photodiode; PBS, polarizing beam splitter; DG, diffraction grating; APD, avalanche photodiode; PCF, photonic crystal fiber; BS, beam splitter. Crystal details appear in Fig. 2.

Mirrors M2 and M3 were concave with -75 mm radius of curvature while mirrors M4 and M5 were planar. The ring cavity confined the oscillating wave to a 27-µm ($1/e^2$) beam radius inside the PPKTP crystal at a signal wavelength of 1.25 µm. The pump laser beam was focused with an f = 63 mm lens through M2 to produce a beam waist radius of 17 µm, as required by the Boyd-Kleinman condition [27]. The PPKTP crystal (see Fig. 2) was 1.2-mm thick with an aperture of 1 × 13 mm, and contained a 1 mm section phasematched for signal generation from 1.0-1.6 µm, a 50 µm section for second-harmonic generation (SHG) of the signal and a 100 µm section for pump-idler sum-frequency generation (SFG). This crystal design enabled the efficient production of pump-idler SFG light, which was heterodyned with common wavelengths in a pump super-continuum (SC) generated in a 30 cm length of photonic crystal fiber (PCF) to yield the idler CEO frequency employed for comb stabilization.

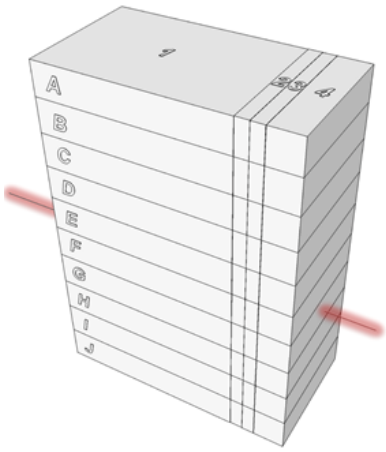

	Λ_1	Λ_2	Λ_3	Λ_4
	(µm)			
A	25.4	6.8	–	21.1
B	25.9	7.1	–	21.0
C	26.4	7.5	–	20.5
D	26.9	8.2	–	20.0
E	27.15	9.0	–	19.0
F	27.25	10.0	–	18.0
G	27.1	11.8	–	16.4
H	26.85	–	–	14.5
I	26.6	18.2	18.2	12.5
J	26.5	23.0	23.0	10.5

Fig. 2. PPKTP crystal design, comprising four sections with lengths of 1 mm, 50 µm, 50 µm and 100 µm. Sections 1, 2 and 4 were phasematched for OPO, signal SHG and pump + idler SFG respectively, with Section 3 being unpoled except for Gratings I and J, in which it was phasematched for signal SHG.

The inclusion of a quasi-phasematched pump-idler SFG section was critical for generating a sufficiently strong signal for idler CEO stabilization, which typically requires a > 30 dB heterodyne beat between the pump supercontinuum and the SFG light. In previously reported examples of OPO frequency-comb locking schemes, parasitic SFM has served this purpose, however it cannot be relied on to be generated with uniform efficiency across a broad tuning range, because it typically originates either from the last coherence length of the crystal or from serendipitous high-order phasematching, which is strongly wavelength dependent. To illustrate the value of incorporating a phasematched SFM section in the crystal design we present in Fig. 3 a simulation of the OPO using a nonlinear envelope equation model [28]. The simulation reached steady state after approximately 80 round-trips, and the evolution of the fields as they propagated the 1.2 mm distance through the crystal is shown for the steady-state condition. This analysis reveals immediately that the pump + idler SFG light is only weakly generated in the OPO section of the crystal (the first 1000 µm), with forward and back conversion over one coherence length being visible (Fig. 3, left plot). Strong SFG is generated in the 50-µm SHG section at 1000 µm and in the 100-µm SFG section at 1100 µm, with the 50-µm blank section at 1050 µm leaving the SFG power unchanged. The inclusion of the SHG/SFG sections therefore enhances the power in the SFG light by nearly two orders of magnitude. While the short grating length limits the absolute power to ~1 mW, this is sufficient to ensure a strong signal is available for CEO locking.

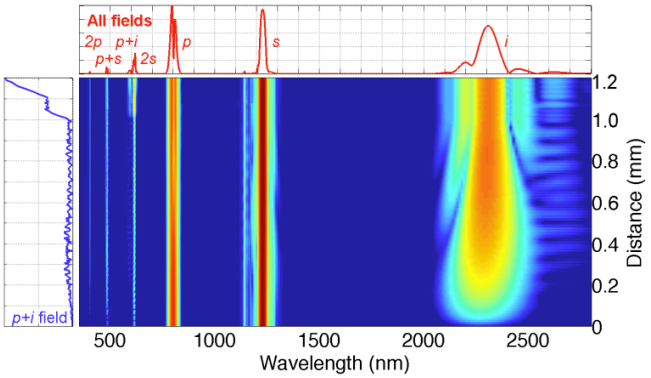

Fig. 3. Simulated OPO output spectrum for Grating G, expressed as a logarithmic density plot, showing its evolution through the crystal once steady-state has been reached. The upper line plot shows, on a linear scale, the fundamental, second-harmonic and sum-frequency fields of the pump (p), signal (s) and idler (i) waves. The line plot left of the main figure shows the evolution of the p + i sum-frequency field, illustrating how its amplitude is enhanced substantially by the inclusion of both the SHG and SFG gratings.

The idler pulses were output coupled through cavity mirror M3 and their tunability was evaluated by directing the collimated idler beam into a Fourier-transform spectrometer. A second beam from a 632.8-nm HeNe laser was coupled into the interferometer for absolute delay calibration. Mid-IR and HeNe calibration interferograms were recorded, with idler spectra measured as the OPO cavity length was tuned. Operation close to degeneracy was unstable and unsuitable for comb stabilization. We note however that, with suitable intracavity dispersion control and cavity stabilization, degenerate femtosecond OPOs can operate stably over a broad instantaneous bandwidth [29-31]. Figure 4 shows the idler spectra for the 1.95–4.0 µm tuning range over which frequency-comb stabilization was possible.

The comb stabilization scheme is illustrated in Fig. 5. The pump repetition rate (f_{REP}) was acquired with a fast Si photodiode (PD) and the sixth harmonic (2 GHz) was isolated with a band-pass filter (BPF).

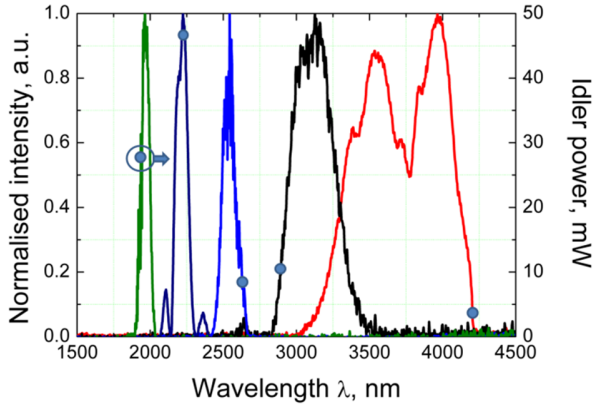

Fig. 4. Cavity-length-tuned OPO idler spectra measured using a Fourier-transform spectrometer. Symbols specify average output coupled idler power.

The detected 2-GHz frequency was mixed with a 2-GHz reference ($f_{REP(REF)}$) from a synthesized signal generator (SSG1) and then low-pass-filtered before entering a proportional-integral (PI) amplifier as an error signal used to actuate a piezoelectric transducer (PZT1) in the Ti:sapphire laser. The stabilized repetition rate could remain locked for 2–3 hours without additional cavity length adjustments.

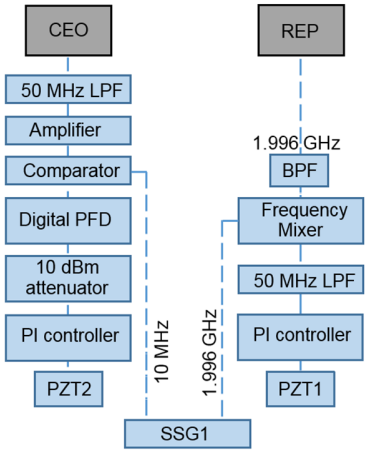

Fig. 5. Comb stabilization scheme, showing the separate control loops used for f_{CEO} and f_{REP} locking.

The CEO frequency of the idler pulses was acquired by heterodyning phasematched pump-idler SFG light with a coherent pump super-continuum [23]. The pump-idler output tuned from 570–670 nm, a wavelength range that could be easily overlapped with the pump super-continuum to provide a CEO beat note for any idler wavelength, as shown in Fig. 6. A monochromator was introduced to select only wavelengths common to both the SC and SFG light, allowing the f_{CEO} signal-to-noise ratio to be maintained at a high level (>35 dB) across the OPO tuning range.

Several components of the system required optimization to maintain the heterodyne beat signal strength as the idler wavelength was tuned. The diffraction grating angle was tuned to ensure that overlapping spectral regions of the pump SC and SFG light remained coincident on the APD. The overlapping spectral regions also travelled with different group velocities in each arm of the interferometer, therefore the relative position of the delay line was adjusted simultaneously as the OPO wavelength was changed. For fine control of the beat signal strength a half-wave plate placed before the PCF was rotated so that the strongest component of the super-continuum overlapped with the pump-idler SFG light from OPO.

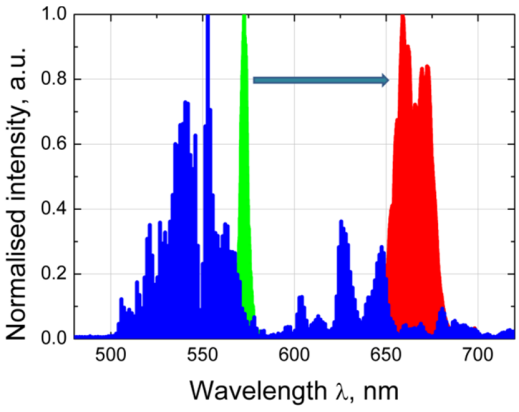

Fig. 6. Spectral overlap of the pump-idler SFG light (green to red) and the pump super-continuum (blue). The 570-nm SFG light (green) was overlapped with the super-continuum light component on one edge giving the CEO frequency of the idler pulse at 1.95 µm. Similarly, the 670-nm SFG light (red) on other edge was overlapped with the super-continuum component for CEO stabilization of the idler at 4.0 µm.

The detected CEO frequency provided an input to one channel of a phase frequency detector (PFD) and was locked to an external 10-MHz rubidium (Rb) clock via a PI amplifier which provided an error signal used to actuate PZT2 in the OPO cavity for f_{CEO} control. Phase-noise measurements of the locked f_{CEO} were carried out by acquiring the PFD output signal with a 12-bit DAQ card. Figure 7 shows the RF spectrum of the stabilized CEO beat note against a 10-MHz reference frequency, recorded using an instrument limited -3-dB bandwidth of 10 Hz and a span of 400 Hz. The CEO-frequency phase-noise power spectral density (PSD) was recorded at regular intervals as the idler was tuned from 1.95–4.0 µm, and a representative measurement (blue) is shown in Fig. 8. The integrated phase noise from 1 Hz–64 kHz was around 1.2 rad, and the upper and lower bounds across the entire idler tuning range are shown in red, indicating a primary contribution arising in the 25–35 kHz range. This noise increase was caused by intensity fluctuations in the pump source for the Ti:sapphire laser which coupled into the OPO as both intensity and phase noise [32]. These fluctuations lay outside the bandwidth of our locking loop, which was limited to 3 kHz by the response of PZT2.

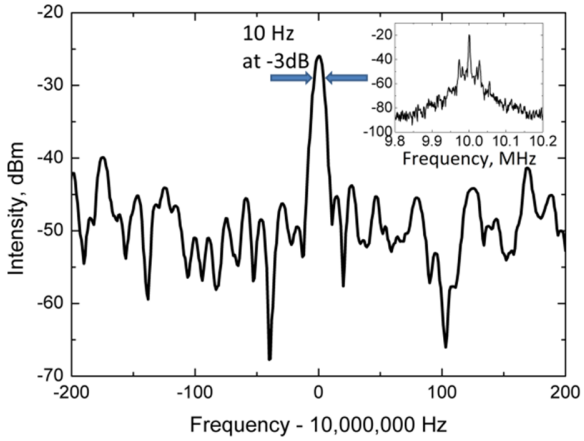

Fig. 7. RF spectrum of the locked idler f_{CEO} recorded with an instrument-limited 10-Hz resolution bandwidth. Inset: 400-kHz bandwidth scan showing locked f_{CEO} with 25–35 kHz sidebands.

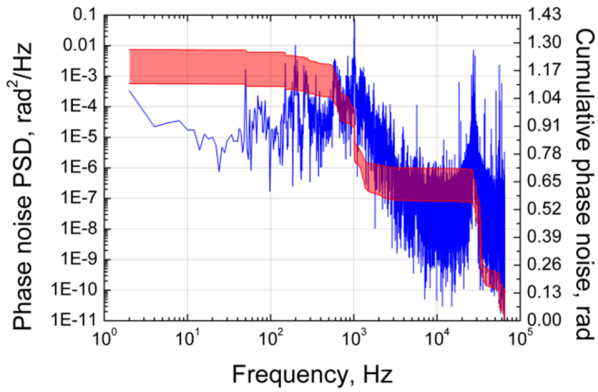

Fig. 8. Characteristic in-loop phase noise PSD for the idler CEO frequency (blue) from 1 Hz–64 kHz (1 second observation time). Upper and lower bounds for the cumulative phase noise across the entire idler tuning are shown in red.

In summary, by combining an optimized nonlinear interferometer with a multi-section PPKTP crystal producing pump-idler SFG powers far exceeding those typically available from only parasitic SFG, we have demonstrated continuously tunable comb operation across >2000 nm in the mid-IR, enabling flexible spectroscopy / metrology in this region.

European Research Council (ERC) (605057).

References

1. Z. Zhang, T. Gardiner, and D. T. Reid, Opt. Lett. **38**, 3148 (2013).
2. K. A. Tillman, R. R. J. Maier, D. T. Reid, and E. D. McNaghten, Appl. Phys. Lett. **85**, 3366 (2004).
3. F. Keilmann, C. Gohle, and R. Holzwarth, Opt. Lett. **29**, 1542 (2004).
4. F. Adler, P. Masłowski, A. Foltynowicz, K. C. Cossel, T. C. Briles, I. Hartl, and J. Ye, Opt. Express **18**, 21861 (2010).
5. W. D. Kimura, A. van Steenbergen, M. Babzien, I. Ben-Zvi, L. P. Campbell, D. B. Cline, C. E. Dilley, J. C. Gallardo, S. C. Gottschalk, P. He, K. P. Kusche, Y. Liu, R. H. Pantell, I. V. Pogorelsky, D. C. Quimby, J. Skaritka, L. C. Steinhauer, and V. Yakimenko, Phys. Rev. Lett. **86**, 4041 (2001).
6. E. Gagnon, I. Thomann, A. Paul, A. L. Lytle, S. Backus, M. M. Murnane, H. C. Kapteyn, and A. S. Sandhu, Opt. Lett. **31**, 1866 (2006).
7. A. Baltuška, T. Fuji, and T. Kobayashi, Phys. Rev. Lett. **88**, 133901 (2002).
8. M. Hentschel, R. Kienberger, C. Spielmann, G. A. Reider, N. Milosevic, T. Brabec, P. Corkum, U. Heinzmann, M. Drescher, and F. Krausz, Nature **414**, 509 (2001).
9. R. Kienberger, E. Goulielmakis, M. Uiberacker, A. Baltuška, V. Yakovlev, F. Bammer, A. Scrinzi, T. Westerwalbesloh, U. Kleineberg, U. Heinzmann, M. Drescher, and F. Krausz, Nature **427**, 817 (2004).
10. A. Gambetta, N. Coluccelli, M. Cassinerio, D. Gatti, P. Laporta, G. Galzerano, and M. Marangoni, Opt. Lett. **38**, 1155 (2013).
11. F. Zhu, H. Hundertmark, A. A. Kolomenskii, J. Strohaber, R. Holzwarth, and H. A. Schuessler, Opt. Lett. **38**, 2360 (2013).
12. C. Erny, K. Moutzouris, J. Biegert, D. Kühlke, F. Adler, A. Leitenstorfer, and U. Keller, Opt. Lett. **32**, 1138 (2007).
13. T. J. Kippenberg, R. Holzwarth, and S. A. Diddams, Science **332**, 555 (2011).
14. P. Del'Haye, A. Schliesser, O. Arcizet, T. Wilken, R. Holzwarth, and T. J. Kippenberg, Nature **450**, 1214 (2007).
15. C. Y. Wang, T. Herr, P. Del'Haye, A. Schliesser, J. Hofer, R. Holzwarth, T. W. Hänsch, N. Picqué, and T. J. Kippenberg, Nat. Commun. **4**, 1345 (2013).
16. A. G. Griffith, R. K. W. Lau, J. Cardenas, Y. Okawachi, A. Mohanty, R. Fain, Y. H. D. Lee, M. Yu, C. T. Phare, C. B. Poitras, A. L. Gaeta, and M. Lipson, Nat. Commun. **6**, (2015).
17. M. N. Cizmeciyan, H. Cankaya, A. Kurt, and A. Sennaroglu, Opt. Lett. **34**, 3056 (2009).
18. E. Sorokin, I. T. Sorokina, J. Mandon, G. Guelachvili, and N. Picqué, Opt. Express **15**, 16540 (2007).
19. E. Sorokin, N. Tolstik, K. I. Schaffers, and I. T. Sorokina, Opt. Express **20**, 28947 (2012).
20. Q. Wang, J. Geng, Z. Jiang, T. Luo, and S. Jiang, IEEE Photon. Tech. Lett. **23**, 682 (2011).
21. C.-C. Lee, C. Mohr, J. Bethge, S. Suzuki, M.E. Fermann, I. Hartl, and T. R. Schibli, Opt. Lett. **37**, 3084 (2012).
22. K. F. Lee, J. Jiang, C. Mohr, J. Bethge, M. E. Fermann, N. Leindecker, K. L. Vodopyanov, P. G. Schunemann, and I. Hartl, Opt. Lett. **38**, 1191 (2013).
23. J. H. Sun, B. J. S. Gale, and D. T. Reid, Opt. Lett. **32**(11), 1414 (2007).
24. F. Adler, K. C. Cossel, M. J. Thorpe, I. Hartl, M. E. Fermann, and J. Ye, Opt. Lett. **34**, 1330 (2009).
25. T. I. Ferreiro, J. Sun, and D. T. Reid, Opt. Express **19**, 24159 (2011).
26. N. Leindecker, A. Marandi, R. L. Byer, and K. L. Vodopyanov, Opt. Express **19**, 6296 (2011).
27. G. D. Boyd and D. A. Kleinman, J. Appl. Phys. **39**, 3597 (1968).
28. D. T. Reid, Opt. Express **19**, 17979–17984 (2011).
29. S. T. Wong, K. L. Vodopyanov, and R. L. Byer, J. Opt. Soc. Am. B **27**, 876 (2010).
30. S. T. Wong, T. Plettner, K. L. Vodopyanov, K. Urbanek, M. Digonnet, and R. L. Byer, Opt. Lett. **33**, 1896 (2008).
31. R. A. McCracken and D. T. Reid, "Few-cycle near-infrared pulses from a degenerat 1-GHz optical parametric oscillator," Opt. Lett., doc. ID 243046 (posted 11 August 2005, in press).
32. T. D. Mulder, R. P. Scott, and B. H. Kolner, Opt. Express **16**, 14186 (2008).

References

1. Z. Zhang, T. Gardiner, and D. T. Reid, "Mid-infrared dual-comb spectroscopy with an optical parametric oscillator," Opt. Lett. **38**, 3148 (2013).
2. K. A. Tillman, R. R. J. Maier, D. T. Reid, and E. D. McNaghten, "Mid-infrared absorption spectroscopy across a 14.4 THz spectral range using a broadband femtosecond optical parametric oscillator," Appl. Phys. Lett. **85**, 3366 (2004).
3. F. Keilmann, C. Gohle, and R. Holzwarth, "Time-domain mid-infrared frequency-comb spectrometer," Opt. Lett. **29**, 1542 (2004).
4. F. Adler, P. Masłowski, A. Foltynowicz, K. C. Cossel, T. C. Briles, I. Hartl, and J. Ye, "Mid-infrared Fourier transform spectroscopy with a broadband frequency comb," Opt. Express **18**, 21861 (2010).
5. W. D. Kimura, A. van Steenbergen, M. Babzien, I. Ben-Zvi, L. P. Campbell, D. B. Cline, C. E. Dilley, J. C. Gallardo, S. C. Gottschalk, P. He, K. P. Kusche, Y. Liu, R. H. Pantell, I. V. Pogorelsky, D. C. Quimby, J. Skaritka, L. C. Steinhauer, and V. Yakimenko, "First Staging of Two Laser Accelerators," Phys. Rev. Lett. **86**, 4041 (2001).
6. E. Gagnon, I. Thomann, A. Paul, A. L. Lytle, S. Backus, M. M. Murnane, H. C. Kapteyn, and A. S. Sandhu, "Carrier-envelope phase shift caused by variation of grating separation," Opt. Lett. **31**, 1866 (2006).
7. A. Baltuška, T. Fuji, and T. Kobayashi, "Controlling the Carrier-Envelope Phase of Ultrashort Light Pulses with Optical Parametric Amplifiers," Phys. Rev. Lett. **88**, 133901 (2002).
8. M. Hentschel, R. Kienberger, C. Spielmann, G. A. Reider, N. Milosevic, T. Brabec, P. Corkum, U. Heinzmann, M. Drescher, and F. Krausz, "Attosecond metrology," Nature **414**, 509 (2001).
9. R. Kienberger, E. Goulielmakis, M. Uiberacker, A. Baltuška, V. Yakovlev, F. Bammer, A. Scrinzi, T. Westerwalbesloh, U. Kleineberg, U. Heinzmann, M. Drescher, and F. Krausz, "Atomic transient recorder," Nature **427**, 817 (2004).
10. A. Gambetta, N. Coluccelli, M. Cassinerio, D. Gatti, P. Laporta, G. Galzerano, and M. Marangoni, "Milliwatt-level-frequency combs in the 8-14 µm range via difference frequency generation from an Er:fiber oscillator," Opt. Lett. **38**, 1155 (2013).
11. F. Zhu, H. Hundertmark, A. A. Kolomenskii, J. Strohaber, R. Holzwarth, and H. A. Schuessler, "High-power mid-infrared frequency comb source based on a femtosecond Er:fiber oscillator," Opt. Lett. **38**, 2360 (2013).
12. C. Erny, K. Moutzouris, J. Biegert, D. Kühlke, F. Adler, A. Leitenstorfer, and U. Keller, "Mid-infrared difference-frequency generation of ultrashort pulses tunable between 3.2 and 4.8 µm from a compact fiber source," Opt. Lett. **32**, 1138 (2007).
13. T. J. Kippenberg, R. Holzwarth, and S. A. Diddams, "Microresonator-Based Optical Frequency Combs," Science **332**, 555 (2011).
14. P. Del'Haye, A. Schliesser, O. Arcizet, T. Wilken, R. Holzwarth, and T. J. Kippenberg, "Optical frequency comb generation from a monolithic microresonator," Nature **450**, 1214 (2007).
15. C. Y. Wang, T. Herr, P. Del'Haye, A. Schliesser, J. Hofer, R. Holzwarth, T. W. Hänsch, N. Picqué, and T. J. Kippenberg, "Mid-infrared optical frequency combs at 2.5 µm based on crystalline microresonator," Nat. Commun. **4**, 1345 (2013).
16. A. G. Griffith, R. K. W. Lau, J. Cardenas, Y. Okawachi, A. Mohanty, R. Fain, Y. H. D. Lee, M. Yu, C. T. Phare, C. B. Poitras, A. L. Gaeta, and M. Lipson, "Silicon-chip mid-infrared frequency comb generation," Nat. Commun. **6**, (2015).
17. M. N. Cizmeciyan, H. Cankaya, A. Kurt, and A. Sennaroglu, "Kerr-lens mode-locked femtosecond Cr^{2+}:ZnSe laser at 2420 nm," Opt. Lett. **34**, 3056 (2009).
18. E. Sorokin, I. T. Sorokina, J. Mandon, G. Guelachvili, and N. Picqué, "Sensitive multiplex spectroscopy in the molecural fingerprint 2.4 µm region with a Cr^{+2}:ZnSe femtosecond laser," Opt. Express **15**, 16540 (2007).
19. E. Sorokin, N. Tolstik, K. I. Schaffers, and I. T. Sorokina, "Femtosecond SESAM-modelocked Cr:ZnS laser," Opt. Express 20, 28947 (2012).
20. Q. Wang, J. Geng, Z. Jiang, T. Luo, and S. Jiang, "Mode-locked Tm-Ho-doped fiber laser at 2.06 µm," IEEE Photon. Tech. Lett. 23, 682 (2011).
21. C.-C. Lee, C. Mohr, J. Bethge, S. Suzuki, M.E. Fermann, I. Hartl, and T. R. Schibli, "Frequency comb stabilization with bandwidth beyond the limit of gain lifetime by an intracavity graphene electro-optic modulator," Opt. Lett. **37**, 3084 (2012).
22. K. F. Lee, J. Jiang, C. Mohr, J. Bethge, M. E. Fermann, N. Leindecker, K. L. Vodopyanov, P. G. Schunemann, and I. Hartl, "Carrier envelope offset frequency of a doubly resonant, nondegenerate, mid-infrared GaAs optical parametric oscillator," Opt. Lett. **38**, 1191 (2013).
23. J. H. Sun, B. J. S. Gale, and D. T. Reid, "Composite frequency comb spanning 0.4-2.4 µm from a phase-controlled femtosecond Ti:sapphire laser and synchronously pumped optical parametric oscillator," Opt. Lett. **32**, 1414 (2007).
24. F. Adler, K. C. Cossel, M. J. Thorpe, I. Hartl, M. E. Fermann, and J. Ye, "Phase-stabilized, 1.5 W frequency comb at 2.8-4.8 µm," Opt. Lett. **34**, 1330 (2009).
25. T. I. Ferreiro, J. Sun, and D. T. Reid, "Frequency stability of a femtosecond optical parametric oscillator frequency comb," Opt. Express **19**, 24159 (2011).
26. N. Leindecker, A. Marandi, R. L. Byer, and K. L. Vodopyanov, "Broadband degenerate OPO for mid-infrared frequency comb generation," Opt. Express **19**, 6296 (2011).
27. G. D. Boyd and D. A. Kleinman, "Parametric Interaction of Focused Gaussian Light Beams," J. Appl. Phys. **39**, 3597 (1968).
28. D. T. Reid, "Ultra-broadband pulse evolution in optical parametric oscillator," Opt. Express **19**, 17979 (2011).
29. S. T. Wong, K. L. Vodopyanov, and R. L. Byer, "Self-phase-locked divide-by-2 optical parametric oscillator as a broadband frequency comb source," J. Opt. Soc. Am. B **27**, 876 (2010).
30. S. T. Wong, T. Plettner, K. L. Vodopyanov, K. Urbanek, M. Digonnet, and R. L. Byer, "Self-phase-locked degenerate femtosecond optical parametric oscillator," Opt. Lett. **33**, 1896 (2008).
31. R. A. McCracken and D. T. Reid, " Few-cycle near-infrared pulses from a degenerat 1-GHz optical parametric oscillator," Opt. Lett., doc. ID 243046 (posted 11 August 2005, in press).
32. T. D. Mulder, R. P. Scott, and B. H. Kolner, "Amplitude and envelope phase noise of a modelocked laser predicted from its noise transfer function and the pump noise power spectrum," Opt. Express **16**, 14186 (2008).